Choi *et al. Applied Biological Chemistry* (2023) 66:92
https://doi.org/10.1186/s13765-023-00850-x

KSABC
The Korean Society for Applied Biological Chemistry

ARTICLE

Open Access

Heterologous expression in *E. coli* and functional characterization of the tomato CPR enzymes

Won Choi[1†], Seo Young Park[1†], Hyun Min Kim[1], Thanh Dat Mai[1], Ju Hui Do[1], Hye Min Jang[1], Hyeon Bae Hwang[1], Eun Gyeong Song[1], Jae Sung Shim[1] and Young Hee Joung[1*]

Abstract

NADPH-cytochrome P450 reductase (CPR) is a key enzyme transferring electrons to cytochrome P450. In tomatoes (*Solanum lycopersicum*), two *CPR* genes, *SlCPR1* and *SlCPR2*, were identified. In all the tested tomato tissues, *SlCPR2* showed higher expression levels than *SlCPR1*. *SlCPR2* expression increased significantly with jasmonic acid treatment. No significant changes were observed with salicylic acid or drought stress treatment. The cDNA of *SlCPRs* were expressed in *Escherichia coli* without any amino acid modification. And the heterologously expressed SlCPR enzymes were reacted with several protein and chemical substrates. SlCPR2 was more active than SlCPR1. Both SlCPR1 and SlCPR2 exhibited strong activity across a pH range of 6.0 to 9.0, with peak activity at pH 8.0. The study opens possibilities for CPR control, biocatalyst development, and exploring oxidase enzyme functions.

Keywords NADPH-cytochrome P450 reductase, Heterologous expression, Enzymatic characterization

Introduction

NADPH-cytochrome P450 reductase (CPR) consists of two domains—one with a binding site for flavin adenine dinucleotide (FAD) and nicotinamide adenine dinucleotide phosphate (NADPH) and another with a binding site for flavin mononucleotide (FMN) [33]. To perform its function, CPR requires the presence of NADPH and the cofactors FAD and FMN. NADPH is the reduced form of NADP + and acts as a cofactor for flavin proteins, and FAD and FMN are flavin proteins that exist in various redox forms and can control electron movement. The electrons provided by NADPH are transferred to FAD and FMN in order, and finally, the electrons required for the reduction reaction are transferred [24, 36]. CPR is known to transfer electrons to diverse enzymes such as oxygenase [9, 14] and fatty acid elongase [10]. It has also been reported to react with various chemicals such as cytochrome b_5 [3], cytochrome *c* [35], 3-(4,5-dimethylthiazol-2-yl)-2,5-diphenyltetrazolium bromide (MTT) [17], 5-cyano-2,3-ditolyltetrazolium chloride (CTC) [15], and ferricyanide [8].

Animals mostly possess a single CPR, which is crucial for normal development and survival. Studies in mice have shown that CPR can induce lethal traits if not expressed properly during embryogenesis [32]. Furthermore, a reduction in CPR expression negatively impacts growth and reproductive capacity [37]. Similarly, in humans, insufficient CPR expression can lead to deterioration in reproductive function. In more severe cases of CPR deficiency, additional complications, such as intellectual disability and abnormalities in skeletal development, may arise [4].

Higher plants have been observed to possess two or three CPRs. Several plant species, including arabidopsis

†Won Choi and Seo Young Park have equally contributed to the project for carrying out experiment, analyses of data, and preparing the manuscript.

*Correspondence:
Young Hee Joung
yhjoung@chonnam.ac.kr
[1] School of Biological Sciences and Technology, Chonnam National University, Gwangju 61186, Republic of Korea

(*Arabidopsis thaliana*) [34], hot pepper (*Capsicum annuum*) [17], Indian ginseng (*Withania somnifera*) [29], cotton (*Gossypium hirsutum*) [38], periwinkle (*Catharanthus roseus*) [26], and legumes (*Medicago truncatula* and *Lotus japonicus*) [11] have two CPRs. Additionally, species such as hybrid poplar [30] and rice (*Oryza sativa*) [27] are known to have three CPRs. It has been hypothesized that, unlike animals, plants have multiple CPRs due to the presence of a greater diversity of oxygenases and their involvement in various biological reactions [30, 35].

Plant CPRs can be classified into two classes: class I and class II. Class I CPR exhibits similar expression patterns in various plant tissues and is mostly involved in primary metabolic processes [12, 34]. Class II CPR has a long membrane anchor at the N-terminus and serves different functions related to plant adaptation and defense responses. Class II CPR is typically induced and upregulated under stress conditions such as pathogen attack and abiotic stresses. Its expression is triggered as part of the plant's defense mechanisms to combat these stresses [21, 26].

Analysis of the tomato genome revealed the presence of two *CPRs*. In this study, we investigated the expression patterns of these two *CPR* genes in tomato tissues and under stress conditions and examined the intercellular localization of these CPRs. To gain a better understanding of the CPR enzymes, we heterologously expressed the enzymes in *Escherichia coli* and isolated. Enzyme characteristics were investigated by confirming their reactivity with various substrates and measuring the protein activity under various conditions.

Materials and methods

Plant culture conditions and stress treatments

Tomato plants (*Solanum lycopersicum* cv. Micro-tom) were grown in the soil of an incubation room maintained at 22–26 °C and 16:8 h light:dark conditions. Tomato roots, leaves, flowers, and fruits at various ripening stages were sampled from more than five plants in one repeat, and a total of three independent repeats were performed. When the fourth true leaves of the tomatoes developed, the plants were sprayed with 80 μM salicylic acid (SA) or 80 μM jasmonic acid (JA) to induce stress responses. As a control group for each experiment, the same amount of water with 0.4% EtOH (SA) or water (JA) was sprayed, and leaves were obtained 1, 3, and 6 h after treatment. Similary, drought stress was treated by stopping irrigation, which was performed three times a week, and tomato plants with 4–5 leaves were used. Subsequently, samples were obtained after 2, 4, and 10 days. These experiments were repeated twice with a pooling of three plants per repeat. Tobacco plants (*Nicotiana benthamiana*) were grown under the same conditions as the tomato plants and were used for subcellular localization of the CPRs 3–4 weeks after germination.

cDNA cloning and quantitative real-time PCR

Total RNA was isolated from tomato tissues using the RNeasy Plant Mini Kit (Qiagen, USA) and cDNA was synthesized using QuantiTect Reverse Transcription Kit (Qiagen, USA) according to the manufacturer's directions. The cDNAs of *SlCPRs* were amplified using specific primer sets (*SlCPR1*; BamHI_SlCPR1_F: 5′—GGA TCC ATG GAG TCG AGT TTG GAG—3′, SlCPR1_SacI_R: 5′—GAG CTC TTA CCA CAC ATC CC—3′, *SlCPR2*; BamHI-SlCPR2_F: 5′—GGA TCC ATG GAT TCT ACA TCA GAA AAG C-3′, SlCPR2_SacI_R: 5′—GAG CTC TTA CCA CAC ATC AC—3′). The synthesized cDNA was cloned into vectors for experiments.

To compare the expression levels of the *SlCPRs* in tomato tissues, real-time PCR was performed using QuantiNova SYBR green kit (QIAGEN, Germany) or AMPIGENE qPCR Green Mix Hi-ROX kit (ENZO, USA) according to the manufacturer's directions. The PCR conditions were as follows: 95 °C for 7 min, followed by 40 cycles at 95 °C for 20 s, 56 °C for 20 s, and 72 °C for 30 s. The tomato actin gene (*ACTIN*, Solyc04g011500) was used as the reference gene. The samples were analyzed in three technical repeats, three biological repeats for various tissue expressions. For analysis of gene expression under stress conditions, *Glucan endo-1,3-beta-glucosidase B* (*SlGluB*) [39], *oxophytodienoate reductase 3* (*SlOPR3*) [23], and *ABA-response element binding factor 1* (*SlAREB1*) [5] were used as marker genes for SA, JA, and drought stress treated, respectively. The samples were analyzed in three technical repeats and two biological repeats for stress response. The mRNA expression levels were normalized and calculated used the comparative C_T method using the housekeeping gene *ACTIN* as an internal control. The primer sets used for this study have similar PCR efficiency. Sequence information of the primers were presented in Additional file 1: Data S2.

Protein tertiary structure prediction

The three-dimensional protein structure of SlCPRs was predicted using the amino acid sequences obtained by translating the tomato cDNA sequence. Analysis of the transmembrane helices was performed using TMHMM-2.0 (Transmembrane prediction using Hidden Markov Models, TMHMM; https://services.healthtech.dtu.dk/services/TMHMM-2.0/). And the SWISS-MODEL (https://swissmodel.expasy.org/interactive) was used for predicting the tertiary structure of the protein, and the template used was one with high sequence identity and coverage among CPRs of other species created by the AlphaFold2 method.

Subcellular localization

Agrobacterium tumefaciens strain GV3101 (GV3101) was transformed with the pBIN recombinant plasmid containing mCherry, showing endoplasmic reticulum (ER)-specific expression, and the pBI121 recombinant plasmid containing enhanced green fluorescent protein (EGFP), SlCPR1-EGFP, and SlCPR2-EGFP (Additional file 1: Data S3), and then cultivated. After primary culture in Yeast Extract Peptone (YEP) media, the bacteria were suspended in 10 mM $MgCl_2$ with 200 μM acetosyringone to obtain a value of 0.7 at OD_{600}. Mixtures of ER-targeting mCherry strains with P19, the silencing suppressor [1], mixed with 35S EGFP, SlCPR1-EGFP, and SlCPR2-EGFP strains, respectively, were used for transient expression (agroinfiltration) through the abaxial side of tobacco leaves using a 1 mL needless syringe.

Three days after tobacco transformation using GV3101, tobacco leaves were cut to a size of approximately 1 cm × 1 cm and microscopic specimens were prepared. The fluorescence expressed in cells was confirmed using a spectral confocal laser scanning TCS-SPE (Leica Microsystems, Germany) in a dark room. In the case of EGFP, fluorescence was confirmed under excitation and emission wavelengths of 488 nm and 500–550 nm, respectively. In the case of mCherry, fluorescence was confirmed under excitation and emission wavelengths of 561 nm and 605–630 nm, respectively.

Induction and purification of CPR proteins

To produce SlCPR proteins, the *E. coli* Rosetta (DE3) pLysS strain was transformed individually with the pET (+28a) vector containing each *SlCPR* gene (Additional file 1: Data S3) and incubated with isopropyl β-d-1-thiogalactopyranoside (IPTG) at 32 °C for 24 h. Then, the culture media were centrifuged at 3500 rpm for 30 min at 4 °C to harvest cells. SlCPR proteins were purified following the method presented in a previous study [17]. Proteins were extracted using a 2′5′-ADP-sepharose column (GE Heathcare, USA) and a Biologic LP instrument (Longer Precision Pump, China) and then concentrated using an Amicon Ultra-15 Centrifugal Filter (Millipore, USA). The size of the isolated proteins was confirmed using 8% sodium dodecyl-sulfate polyacrylamide gel electrophoresis (SDS-PAGE), and the concentration of active proteins was determined using cytochrome *c* [6].

Measurement of the reaction between the SlCPR proteins and substrates

To measure activity, CPR and substrates were reacted in the presence of NADPH. The reactions of MTT [17], CTC [15], and ferricyanide [8], the chemical substrates of CPR, with cytochrome *c* [35], a protein substrate, were observed using a spectrophotometer (Shimadzu-UV-1601). A mix containing 10 nM SlCPR protein and substrates (MTT, CTC, or ferricyanide, 0–500 μM; cytochrome *c*, 0–100 μM) in 100 mM potassium phosphate buffer (CTC, pH 7.4; others, pH 7.6) was measured at the wavelength at which each substrate reacted (MTT, 610 nm; CTC, 450 nm; ferricyanide, 420 nm; cytochrome *c*, 550 nm). Then, the amount of reactants formed according to the concentration of each substrate was calculated using the extinction coefficient of each substrate. Kinetic parameters (K_{cat} and K_m) were calculated through nonlinear regression analysis and asymmetric sigmoidal analysis using GraphPad Prism (https://www.graphpad.com/).

pH activity and thermal stability of the SlCPR proteins

To find out the optimal pH range for SlCPR protein activity, a potassium phosphate buffer ranging from pH 6.0 to 9.0 was prepared and the MTT assay was performed. A mixture containing each buffer, 10 μM MTT, and 10 nM SlCPR was placed in a cuvette, which was zeroed at 610 nm using a spectrophotometer, and the absorbance was continuously measured after adding 100 μM NADPH. The reduced MTT formed at each pH was measured and calculated based on the change in absorbance.

The thermal stability of the SlCPR proteins was tested as described previously [17], with slight modifications. The SlCPR proteins were heat-treated at temperatures ranging from 26 °C to 70 °C for 10 min and then at 4 °C for 5 min using PCR equipment before the MTT assay was performed. The activity of the heat-treated proteins was expressed in percentage, with the activity of the protein reacted at 26 °C being 100%.

Results

Isolation of *CPR* genes from tomato

Investigation of the tomato genome database (http://solegenomice.net) confirmed that there are two different *CPRs*—solyc04g076380 and solyc07g019460. The cDNAs of the two genes were isolated from tomato (*S. lycopersicum* cv. Micro-Tom) through RT-PCR.

CPR can be broadly categorized into two classes based on the length of the N-terminal anchor. The group with a 20–30 shorter amino acid anchor is classified as class I, while the other belongs to class II. After translating the amino acid sequence based on the cDNA information of the solyc04g076380 and solyc07g019460 genes and performing alignment analysis using CPR sequences of various plant species, it was determined that solyc04g076380 belongs to class I, whereas solyc07g019460 belongs to class II; therefore, they were named *SlCPR1* and *SlCPR2*, respectively (Fig. 1).

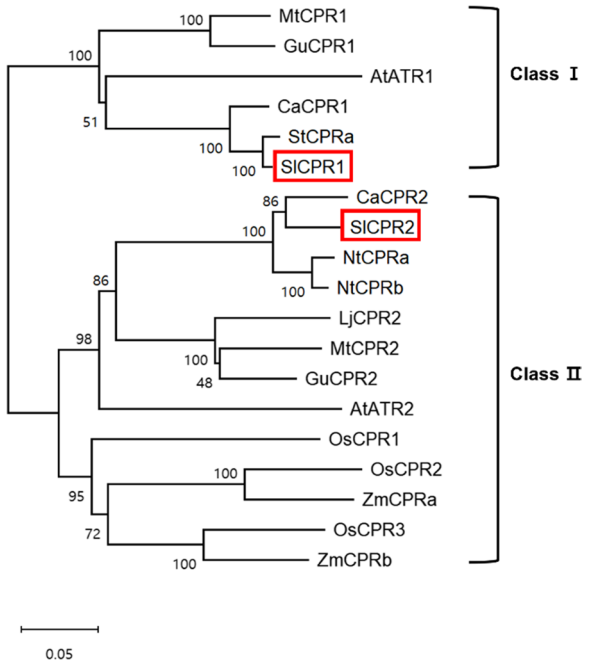

Fig. 1 Phylogenetic analysis of SlCPRs and other reported plant CPRs. The neighbor-joining phylogram was constructed using MEGA X software [16]. The numbers next to each node are bootstrap values from 1000 replicates, and values higher than 50 are indicated.

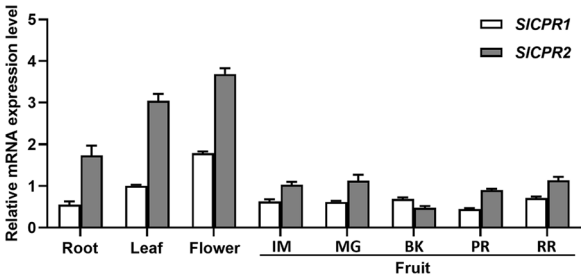

Fig. 2 Relative mRNA expression levels of *SlCPRs* in various tissues and fruit ripening stages. Quantitative real-time PCR was performed using tomato (*S. lycopersicum* cv. Micro-tom) root, leaf, flower, and fruits. Transcript levels were normalized using the tomato *ACTIN* gene as an internal control. Each bar represents the mean and standard error. *IM*, Immature green stage, *MG* Mature green stage, *BK* Breakers stage, *PR* Pink and Red stage, *RR* Ripening Red stage

These two SlCPRs exhibited high similarity to the CPRs found in *Solanaceae* plants. Upon analyzing the functional domains of CPR1 and CPR2, it was observed that the sequences of the FMN, FAD, and NADPH binding domains were highly conserved (Additional file 1: Data S1). This finding indicates that these important functional domains involved in electron transfer are preserved in both SlCPR1 and SlCPR2, suggesting their crucial roles in catalytic activity and interaction with oxygenases.

The NCBI accession numbers of the CPRs are as follows: AtCPR1 (NP_194183), AtCPR2 (NP_194750), CaCPR1 (NP_001311873.1), CaCPR2 (XP_016580172.1), StCPRa (XP_006338052.1), GuCPR1 (AUG98241.1), GuCPR2 (QCZ35624.1), SlCPR1 (XP_004238001.1), SlCPR2 (XP_004242931.1), LjCPR2 (BAG68945.1), MtCPR1 (XP_003602898.1), MtCPR2 (XP_003610109.1), NtCPRa (XP_016436428.1), NtCPRb (XP_016454942.1), OsCPR1 (XP_015636692.1), OsCPR2 (XP_015650780.1), OsCPR3 (XP_015651232.1), ZmCPR1 (NP_001346444.1), and ZmCPRb (XP_008653023.1).

At, Arabidopsis thaliana; Ca, Capsicum annuum; Gu, Glycyrrhiza uralensis; *Sl, Solanum lycopersicum; St, Solanum tuberosum; Lj, Lotus japonicus; Mt, Medicago truncatula; Nt, Nicotiana tabacum; Os, Oryza sativa; Zm, Zea mays.*

Expression levels of *SlCPR1* and *SlCPR2* in tomato

The expression levels of *SlCPR1* and *SlCPR2* were determined through mRNA expression analysis (Fig. 2). In all tested tissues, the expression of *SlCPR2* was higher than that of *SlCPR1*. Both genes displayed higher expression in leaf and flower tissues than in fruits. These results suggest that the two *SlCPR* genes display similar expression patterns but with varying expression levels.

To examine the expression patterns of the two *SlCPR* genes under various conditions, tomato plants were divided into three distinct groups: one group was treated with the stress-related hormone SA, another with the stress-related hormone JA, and a third group was subjected to drought stress. The effectiveness of the different stress treatments was verified using *GluB*, *OPR3*, and *AREB1* as markers for SA, JA, and drought stress, respectively (Fig. 3). *SlCPR1* showed no significant change in expression levels across these stress treatments. On the other hand, *SlCPR2* showed a significant increase in gene expression only under JA treatment, suggesting that JA specifically induces the upregulation of *SlCPR2*.

Structure and subcellular localization of SlCPRs

Analysis of the transmembrane helices of the two proteins and prediction of their tertiary structures revealed that there is a membrane anchor domain at the N-terminus of the amino acid sequences of the SlCPRs (Additional file 1: Data S4, Fig. 4A). Thus, the subcellular localization of CPR was determined by fusing EGFP to the C-terminal end of CPR. The experimental results showed that the CPR-EGFP fusion protein was predominantly localized on the ER membrane, supporting the

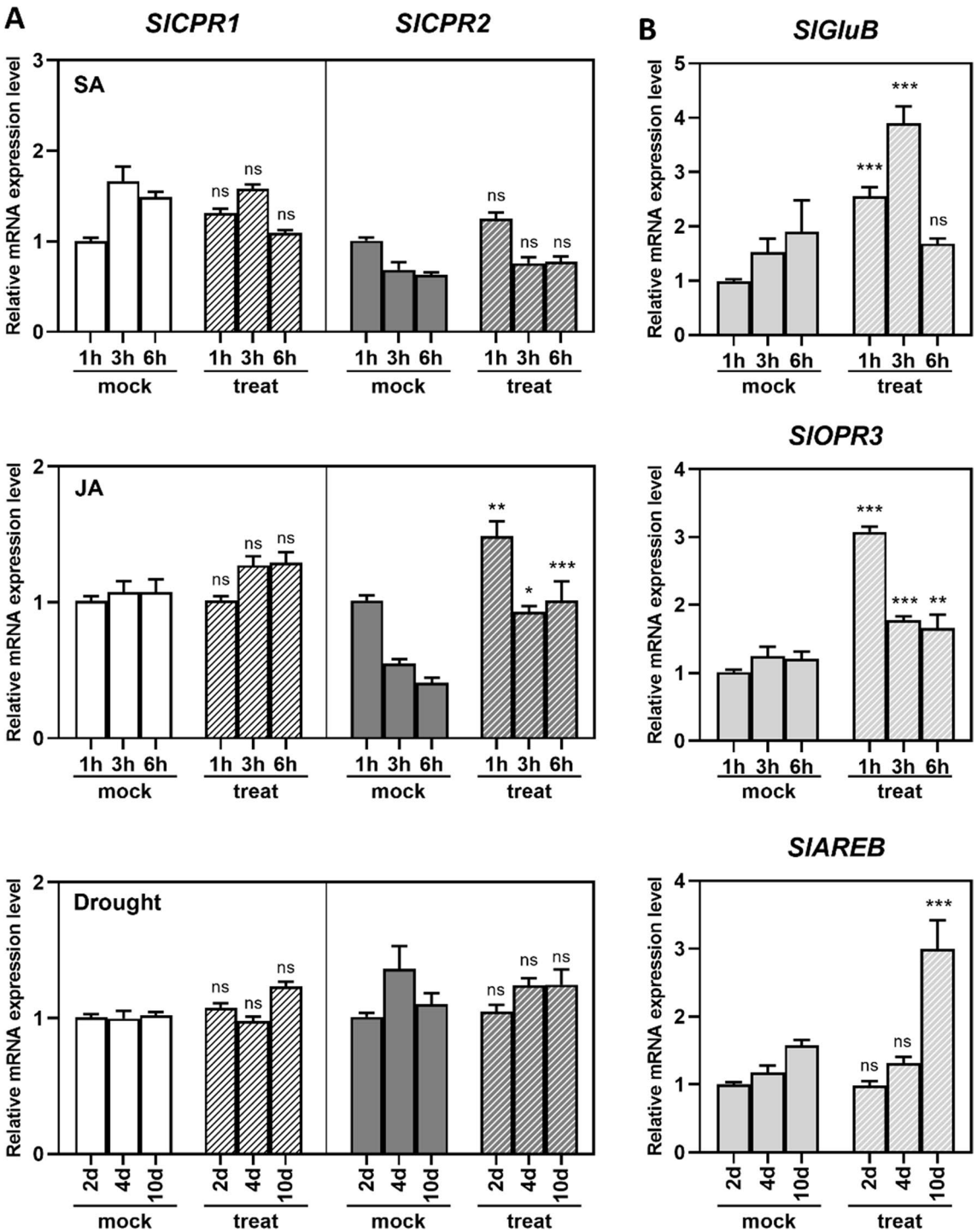

Fig. 3 Relative mRNA expression levels of *SlCPRs* in tomato leaves under stress conditions. Expression patterns of *SlCPRs* **A**, and each stress marker gene **B** in stress-treated tomatoes. The transcript levels of the stress-treated samples were normalized using the tomato *ACTIN* gene as an internal control. Each reaction was expressed as a relative value for 1 h of mock (SA or JA) or 2 days of mock (drought). Each bar represents the mean and standard error. ANOVA was tested using the Bonferroni method and marked as follows: ns, $p > 0.05$; *, $p < 0.05$; **, $p < 0.01$; ***, $p < 0.001$.

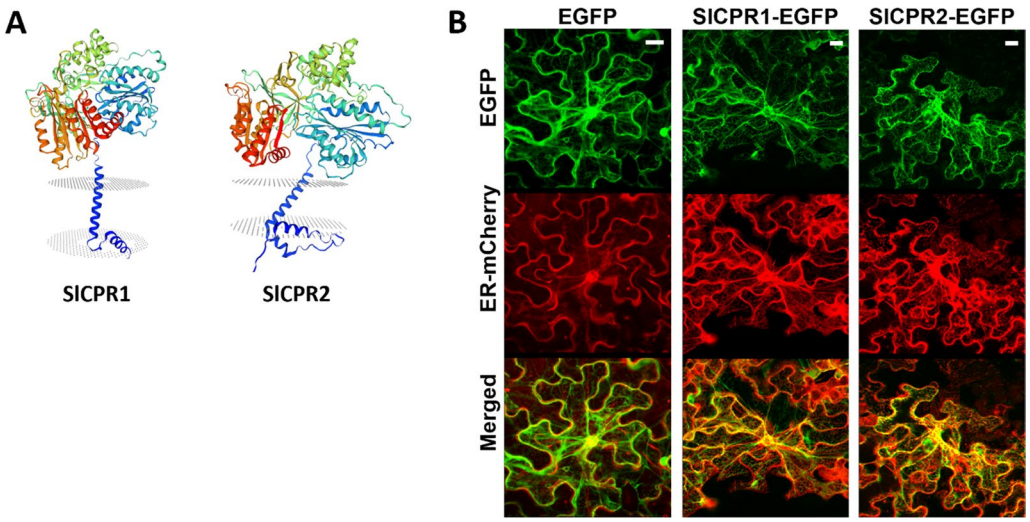

Fig. 4 Tertiary structure prediction and subcellular localization in tobaccos of SlCPRs. **A**, Diagrams presenting the predicted tertiary structures of the two SlCPRs. The protein structures were predicted using SWISS-MODEL, with a rainbow coloring gradient from the N-terminal (blue) to the C-terminal (red). The predicted transmembrane sites are indicated using gray dots. **B**, Confocal microscopy images of *N. benthamiana* epidermal cells. A 35S promoter was used for all vectors, and CPRs were linked to the N-terminus of EGFP and expressed (in green). The endoplasmic reticulum was labeled in red. The EGFP and mCherry signals were individually captured through the green and red channels, respectively. Yellow in the overlay images indicates co-localization. Scale bar: 20 μm.

hypothesis that CPR exists primarily on the ER membrane (Fig. 4B).

Enzymatic activities of SlCPRs toward substrates

To examine the enzymatic activities, SlCPR1 and SlCPR2 were expressed in *E. coli* and, subsequently, isolated and purified. The membrane fractions containing the SlCPRs were solubilized, and the SlCPR proteins were purified using affinity chromatography. Upon analysis using SDS-PAGE, the purified SlCPR1 protein displayed a band at the expected molecular weight of 76 kDa and the SlCPR2 protein showed a band at the expected molecular weight of 79 kDa (Fig. 5).

To assess the catalytic activity of the SlCPRs, the purified proteins were reacted with substrates such as MTT, CTC, ferricyanide, and cytochrome *c*. The formation of reaction products was measured at various substrate concentrations to calculate the kinetic parameters (Table 1, Additional file 1: Data S5) K_{cat} (turnover number) and K_m (substrate concentration at half-maximal velocity). Both SlCPR1 and SlCPR2 exhibited high K_{cat} with the substrates; K_{cat} was highest with ferricyanide, followed by cytochrome *c*, MTT, and CTC for SlCPR1, and MTT, cytochrome *c*, and CTC for SlCPR2, in that order. SlCPR2 displayed a higher catalytic efficiency (K_{cat}/K_m) than SlCPR1 for all tested substrates. Particularly, when reacted with MTT, SlCPR2 exhibited approximately five times higher catalytic efficiency than SlCPR1. These findings highlight the differential catalytic efficiencies of SlCPR1 and SlCPR2, suggesting variations in their ability to efficiently transfer electrons to different substrates.

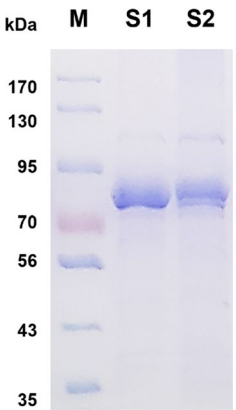

Fig. 5 SDS-PAGE of SlCPR1 and SlCPR2. *Escherichia coli* expressing SlCPR proteins were isolated and SDS-PAGE was performed. The SDS-PAGE gel was stained with Coomassie Brilliant Blue R250. M, protein marker; S1, isolated SlCPR1 protein; S2, isolated SlCPR2 protein.

Table 1 Kinetic parameters of MTT, ferricyanide, CTC, and cytochrome *c* reduction by the SlCPRs

	SlCPR1			SlCPR2		
	***K*cat (s^{-1})**	***K*m (μM)**	***K*cat/*K*m**	***K*cat (s^{-1})**	***K*m (μM)**	***K*cat/*K*m**
MTT	49.4 ± 2.1	26.3 ± 4.1	1.88	147 ± 2.5	13.7 ± 0.92	10.7
CTC	25.3 ± 0.64	20.6 ± 2.1	1.23	30.7 ± 0.95	22.7 ± 2.9	1.35
Ferricyanide	228 ± 6.5	117 ± 9.1	1.95	282 ± 5.6	21.2 ± 1.7	13.3
Cytochrome *c*	51.9 ± 2.1	24.2 ± 1.0*	2.14	91.8 ± 0.81	24.6 ± 0.23*	3.73

Kinetic parameters were studied through the reaction of the two SlCPRs with different concentrations of substrates (MTT, CTC, and ferricyanide, 0–500 μM; cytochrome *c*, 0–100 μM). The values for MTT, CTC, and ferricyanide were calculated through non-linear regression analysis of Michaelis–Menten plots and those for cytochrome *c* were calculated through asymmetric sigmoidal analysis, using the respective substrate coefficients. The values are presented as mean and standard errors of three repeats. *Shows $K_{1/2}$ instead of K_m

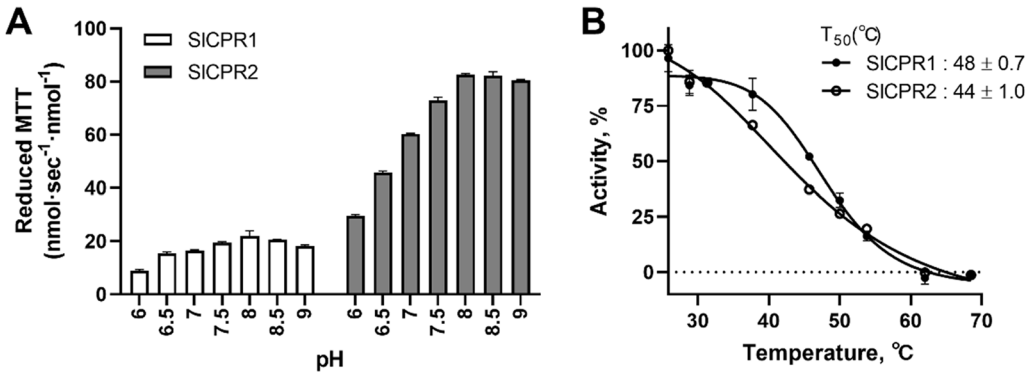

Fig. 6 Effect of pH and temperature on the reactivity of SlCPR1 and SlCPR2 with MTT. **A**, The reactivity of SlCPR1 and SlCPR2 in the pH range of 6.0 to 9.0. **B**, Thermal stability of SlCPR1 and SlCPR2. Proteins were incubated at temperatures ranging from 26 to 70 °C using a PCR device. The activity of the enzymes was presented as 100% when the proteins were reacted at 26 °C. Each bar and dot represents the mean and standard error, respectively.

Optimal pH and thermal stability of the SlCPRs

The reactivity of the SlCPRs with MTT was investigated across a pH range of 6.0 to 9.0 to determine the optimal pH condition for the activity of the two SlCPRs. Both SlCPR1 and SlCPR2 exhibited high activity within this pH range, and their activities gradually increased as the pH increased. The highest activity was observed at around pH 8.0. Importantly, even at pH 9.0, the activity of SlCPR1 was maintained at approximately 83%, and the activity of SlCPR2 was maintained at approximately 97%, compared to that at pH 8.0. These findings demonstrate that both SlCPR1 and SlCPR2 are capable of functioning effectively and maintaining high activity over a wide pH range, indicating their stability and adaptability under different pH conditions (Fig. 6A).

The thermal stability of SlCPR1 was assessed by determining its T_{50} value, which represents the temperature at which the enzyme retains 50% of its activity. The T_{50} values of SlCPR1 and SlCPR2 were determined to be 48 ± 0.7 °C and 44 ± 1.0 °C, respectively. Both SlCPRs exhibited a gradual decrease in activity beyond 30 °C and became completely inactive at 60°C. The thermal stability of the two enzymes was similar (Fig. 6B).

Discussion

The gene expression patterns of *SlCPR1* and *SlCPR2* in different tomato tissues and fruit ripening stages revealed that the two genes displayed similar expression patterns but with varying expression levels. Specifically, the expression of *SlCPR2* was higher than that of *SlCPR1* (Fig. 2). These results differ from those obtained from analyzing *CPR* expression in closely related species such as hot pepper. In hot pepper, the expression of class I CPR (*CaCPR1*) was higher than that of class II CPR (*CaCPR2*) in all tested tissues [17]. Furthermore, heterologous expression of the CaCPR2 did not exhibit activity, unlike SlCPR2 (data not shown). Given that plants have evolved diverse adaptation mechanisms in response to their environment, it is speculated that the characteristics of CPR may differ among closely related species.

The expression patterns of *CPRs* in tomatoes under various stress conditions revealed that the expression

of *SlCPR1* remained largely unchanged, whereas that of *SlCPR2* was induced specifically by JA treatment (Fig. 3). This finding aligns with the characteristics of SlCPR2, which is a class II CPR, in contrast to SlCPR1, which is a class I CPR. Class II CPR is known to play a role in plant adaptation and defense responses [25, 26]. Similar observations have been made in other plant species as well. For instance, in arabidopsis, only the expression of *AtCPR2* increased upon wounding and treatment with herbicides [21, 34]. Similarly, in cotton, the expression of *GhCPR2* was elevated in response to wounding [38]. In Indian ginseng, the expression of *WsCPR2* was strongly induced by methyl JA but only weakly induced by SA [29]. These reports suggest that the expression of class II CPRs can be induced by various stresses, but the stress to which it responds sensitively may vary depending on the species.

Both SlCPR1 and SlCPR2 exhibited high levels of activity across a broad range of pH conditions (Fig. 6). These findings are consistent with those of a previous study that investigated the pH stability of rat CPR and CaCPR1 [17]. The pH stability of CaCPR1 was found to be higher than that of rat CPR. Since pH stability may be related to the structure of the protein, the protein structure of rat CPR was predicted with Alphafold2, and tomato and pepper CPR were predicted with SWISS-MODEL. The structures of the functional domain of electron transfer in the these CPRs are similar to those of SlCPRs shown in Fig. 4. The region that differed significantly was the membrane anchor region preceding the FMN binding domain. The helical structure of the membrane anchor domain of rat CPRs was found to be shorter than that of CaCPRs and SlCPRs. However, changes in protein stability due to structural differences in this region have not yet been clearly studied, so it will be need to investigate the relationship through other studies in the future.

Additionally, the ability of plant CPRs to maintain stability over a wider pH range than animal CPRs may be attributed to the unique characteristics of plant cells. Plant cells contain multiple organelles with varying pH values [2, 7]. pH variations have been observed during specific plant processes, such as root hair growth and pollen tube elongation, stomatal closure in guard cells, and plant–pathogen interactions [28]. The study of pH changes induced by intracellular signals or stress has been conducted in a cell- or tissue-specific manner across various plant species, highlighting the significance of maintaining protein activity under wide pH conditions. The ability of CPR enzymes to maintain stability over a wide pH range holds promise for their industrial applications, especially considering the involvement of partner enzymes in the synthesis of various valuable metabolites.

Moreover, this research opens up possibilities for investigating the functions of numerous oxygenase enzymes, including cytochrome P450s and heme oxygenases. These oxygenases are involved in various biological processes in organisms. In plants, they play an important role in primary and secondary metabolisms, biosynthesis and mechanism of hormones and signal transducers, and defense mechanisms [13, 18–20, 22, 31]. Therefore, the control and manipulation of CPRs acting on oxygenases could be used as a technique to modify various aspects of plant physiology, allowing for the potential editing of plant properties and the development of biocatalysts. These studies can help in the exploration of natural plant compounds with potential applications in medicine, antibiotic alternatives, dietary supplements, and cosmetics. Furthermore, research on the widely utilized crops in the agricultural and livestock industries will contribute to the development of resilient crops capable of withstanding diverse biotic and abiotic stresses, increasing production, or possessing enhanced utility value.

In summary, two *CPR* genes were identified through the sequencing of the tomato genome, and they exhibited conserved FMN, FAD and NADPH binding domain sequences. The expression of *SlCPR2* was induced by JA treatment. Subcellular localization indicated that the SlCPRs were predominantly expressed in the ER of plant cells. The SlCPRs were expressed in *E. coli*, isolated, purified, and reacted with various substrates such as MTT, CTC, ferricyanide, and cytochrome *c*. Both SlCPRs exhibited high activity with the tested substrates, and SlCPR2 showed greater reactivity than SlCPR1. Furthermore, both SlCPRs exhibited high enzymatic activity over a wide range of pH conditions.

Abbreviations

SlCPR	*Solanum lycopersicum* NADPH-cytochrome P450 reductase
CPR	NADPH-cytochrome P450 reductase
CTC	5-Cyano-2,3-ditolyl tetrazolium chloride
MTT	3-(4,5-Dimethylthiazol-2-yl)-2,5-diphenyltetrazolium bromide

Supplementary Information

The online version contains supplementary material available at https://doi.org/10.1186/s13765-023-00850-x.

Additional file 1: Data S1. The amino acid sequence alignment of CPRs. **Data S2.** The primer sequences used for quantitative real-time PCR. **Data S3.** Scheme of the plasmid vectors used in the experiment. **Data S4.** Membrane topology prediction of SlCPRs using the TMHMM program. **Data S5.** Concentration-dependent reduction of MTT **A**, CTC **B**, ferricyanide **C**, and cytochrome c **D** by the SlCPR proteins.

Acknowledgements
Not applicable.

Author contributions
YHJ supervised the research design and wrote the paper; WC and SYP performed biochemical and molecular biology experiments, manuscript editing, TDM, JHD, HBH and EGS performed molecular biology experiments, HMK, HMJ and JSS performed plant physiology experiments.

Funding
This work was supported by a grant from the New Breeding Technologies Development Program (Project No. RD010052 (PJ01654401) to YH, Joung), Rural Development Administration, Republic of Korea.

Availability of data and materials
The datasets used and/or analysed during the current study are available from the corresponding author on reasonable request.

Declarations

Competing interests
The authors declare that they have no competing interests.

Received: 10 October 2023 Accepted: 12 December 2023
Published online: 19 December 2023

References

1. Ahn J-W, Lee JS, Davarpanah SJ, Jeon J-H, Park Y-I, Liu JR, Jeong WJ (2011) Host-dependent suppression of RNA silencing mediated by the viral suppressor p19 in potato. Planta 234:1065–1072
2. Benčina M (2013) Illumination of the spatial order of intracellular pH by genetically encoded pH-sensitive sensors. Sensors 13:16736–16758
3. Enoch HG, Strittmatter P (1979) Cytochrome b5 reduction by NADPH-cytochrome P-450 reductase. J Biol Chem 254:8976–8981
4. Flück CE, Pandey AV (2011) Clinical and biochemical consequences of p450 oxidoreductase deficiency. Pediatric Adrenal Diseases 20:63–79
5. Gao Y-F, Liu J-K, Yang F-M, Zhang G-Y, Wang D, Zhang L, Ou Y-B, Yao Y-A (2020) The WRKY transcription factor WRKY8 promotes resistance to pathogen infection and mediates drought and salt stress tolerance in Solanum lycopersicum. Physiol Plant 168:98–117
6. Guengerich FP, Martin MV, Sohl CD, Cheng Q (2009) Measurement of cytochrome P450 and NADPH–cytochrome P450 reductase. Nat Protoc 4:1245–1251
7. Guern J, Felle H, Mathieu Y, Kurkdjian A (1991) Regulation of intracellular pH in plant cells. Int Rev Cytol 127:111–173
8. Hamdane D, Xia C, Im S-C, Zhang H, Kim J-JP, Waskell L (2009) Structure and function of an NADPH-cytochrome P450 oxidoreductase in an open conformation capable of reducing cytochrome P450. J Biol Chem 284:11374–11384
9. Hannemann F, Bichet A, Ewen KM, Bernhardt R (2007) Cytochrome P450 systems—biological variations of electron transport chains. Biochimica et Biophys Acta General Subjects 1770:330–344
10. Ilan Z, Ilan R, Cinti DL (1981) Evidence for a new physiological role of hepatic NADPH:ferricytochrome (P-450) oxidoreductase. direct electron input to the microsomal fatty acid chain elongation system. J Biol Chem 256:10066–10072
11. Istiandari P, Yasumoto S, Srisawat P, Tamura K, Chikugo A, Suzuki H, Seki H, Fukushima EO, Muranaka T (2021) Comparative analysis of NADPH-cytochrome P450 reductases from legumes for heterologous production of triterpenoids in transgenic *Saccharomyces* cerevisiae. Front Plant Sci. https://doi.org/10.3389/fpls.2021.762546
12. Jensen K, Møller BL (2010) Plant NADPH-cytochrome P450 oxidoreductases. Phytochemistry 71:132–141
13. Kahn RA, Durst F (2000) Function and evolution of plant cytochrome P450. Recent Adv Phytochem 34:151–190
14. Kikuchi G, Yoshida T, Noguchi M (2005) Heme oxygenase and heme degradation. Biochem Biophys Res Commun 338:558–567
15. Kim D-H, Yim S-K, Kim K-H, Ahn T, Yun C-H (2009) Continuous spectrofluorometric and spectrophotometric assays for NADPH-cytochrome P450 reductase activity using 5-cyano-2,3-ditolyl tetrazolium chloride. Biotech Lett 31:271–275
16. Kumar S, Stecher G, Li M, Knyaz C, Tamura K (2018) MEGA X: molecular evolutionary genetics analysis across computing platforms. Mol Biol Evol 35:1547–1549
17. Lee G-Y, Kim HM, Ma SH, Park SH, Joung YH, Yun C-H (2014) Heterologous expression and functional characterization of the NADPH-cytochrome P450 reductase from *Capsicum annuum*. Plant Physiol Biochem 82:116–122
18. Li L, Lin S, Chen Y, Wang Y, Xiao L, Ye X, Sun L, Zhan R, Xu H (2022) Cytochrome P450 monooxygenase/cytochrome P450 reductase bi-enzymatic system isolated from Ilex asprella for regio-specific oxidation of pentacyclic triterpenoids. Front Plant Sci. https://doi.org/10.3389/fpls.2022.831401
19. Liu J, Tian M, Wang Z, Xiao F, Huang X, Shan Y (2022) Production of hesperetin from naringenin in an engineered *Escherichia* coli consortium. J Biotechnol 347:67–76
20. Mitchell AJ, Weng J-K (2019) Unleashing the synthetic power of plant oxygenases: from mechanism to application. Plant Physiol 179:813–829
21. Mizutani M, Ohta D (1998) Two isoforms of NADPH: cytochrome P450 reductase in *Arabidopsis* thaliana: gene structure, heterologous expression in insect cells, and differential regulation. Plant Physiol 116:357–367
22. Mizutani M, Ohta D (2010) Diversification of P450 genes during land plant evolution. Annu Rev Plant Biol 61:291–315
23. Müssig C, Biesgen C, Lisso J, Uwer U, Weiler EW, Altmann T (2000) A novel stress-inducible 12-oxophytodienoate reductase from Arabidopsis thaliana provides a potential link between Brassinosteroid-action and Jasmonic-acid synthesis. J Plant Physiol 157:143–152
24. Murataliev MB, Feyereisen R, Walker FA (2004) Electron transfer by diflavin reductases. Biochimica et Biophys Acta Roteins Proteom 1698:1–26
25. Paquette SM, Jensen K, Bak S (2009) A web-based resource for the Arabidopsis P450, cytochromes b5, NADPH-cytochrome P450 reductases, and family 1 glycosyltransferases. Phytochemistry 70:1940–1947
26. Parage C, Foureau E, Kellner F, Burlat V, Mahroug S, Lanoue A, Dugé de Bernonville T, Londono MA, Carqueijeiro I, Oudin A et al (2016) Class II cytochrome P450 reductase governs the biosynthesis of alkaloids. Plant Physiol 172:1563–1577
27. Park S, Kim Y-S, Rupasinghe SG, Schuler MA, Back K (2013) Rice P450 reductases differentially affect P450-mediated metabolism in bacterial expression systems. Bioprocess Biosyst Eng 36:325–331
28. Raghavendra AS, Ye W, Kinoshita T (2023) Editorial: pH as a signal and secondary messenger in plant cells. Front Plant Sci 14:1148689
29. Rana S, Lattoo SK, Dhar N, Razdan S, Bhat WW, Dhar RS, Vishwakarma R (2013) NADPH-cytochrome P450 reductase: molecular cloning and functional characterization of two paralogs from *Withania somnifera* (L) dunal. PLOS ONE 8:e57068
30. Ro D-K, Ehlting J, Douglas CJ (2002) Cloning, functional expression, and subcellular localization of multiple NADPH-cytochrome P450 reductases from hybrid poplar. Plant Physiol 130:1837–1851
31. Shekhawat GS, Verma K (2010) Haem oxygenase (HO): an overlooked enzyme of plant metabolism and defence. J Exp Bot 61:2255–2270
32. Shen AL, O'Leary KA, Kasper CB (2002) Association of multiple developmental defects and embryonic lethality with loss of microsomal NADPH-cytochrome P450 oxidoreductase. J Biol Chem 277:6536–6541
33. Smith GC, Tew DG, Wolf CR (1994) Dissection of NADPH-cytochrome P450 oxidoreductase into distinct functional domains. Proc Natl Acad Sci 91:8710–8714
34. Sundin L, Vanholme R, Geerinck J, Goeminne G, Höfer R, Kim H, Ralph J, Boerjan W (2014) Mutation of the inducible ARABIDOPSIS THALIANA CYTOCHROME P450 REDUCTASE2 alters lignin composition and improves saccharification. Plant Physiol 166:1956–1971
35. Urban P, Mignotte C, Kazmaier M, Delorme F, Pompon D (1997) Cloning, yeast expression, and characterization of the coupling of two distantly related *Arabidopsis thaliana* NADPH-cytochrome P450 reductases with P450 CYP73A5. J Biol Chem 272:19176–19186
36. Vermilion JL, Coon MJ (1978) Purified liver microsomal NADPH-cytochrome P-450 reductase spectral characterization of oxidation-reduction states. J Biol Chem 253:2694–2704
37. Wu L, Gu J, Cui H, Zhang Q-Y, Behr M, Fang C, Weng Y, Kluetzman K, Swiatek PJ, Yang W et al (2005) Transgenic mice with a hypomorphic NADPH-cytochrome P450 reductase gene: effects on development, reproduction, and microsomal cytochrome P450. J Pharmacol Exp Ther 312:35–43
38. Yang C-Q, Lu S, Mao Y-B, Wang L-J, Chen X-Y (2010) Characterization of two NADPH: Cytochrome P450 reductases from cotton (*Gossypium hirsutum*). Phytochemistry 71:27–35
39. Zhang H, Zhang D, Chen J, Yang Y, Huang Z, Huang D, Wang X-C, Huang R (2004) Tomato stress-responsive factor TSRF1 interacts with ethylene

responsive element GCC box and regulates pathogen resistance to *Ralstonia solanacearum*. Plant Mol Biol 55:825–834

Publisher's Note